Supplementary Information (SI)

Tuning aerogel morphology by water – ionic liquid binary mixtures: a mechanistic journey from the synthesis to the carbon properties

Dávid Nyul, Krisztina László, Oldamur Hollóczki, Mónika Kéri*

Background of cryoporometry measurements:

Modified Gibbs-Thomson equation:[1]

$$T_{m/f} - T_0 = -\frac{V_M \times \gamma_{sl} \times T_0}{\Delta H} \times \frac{S}{V} = -K_c \times \frac{S}{V} = -\frac{nK_c}{r_p} \quad \text{Eq. S1}$$

where $T_{m/f}$ is the melting and freezing point of the liquid in the porous system, T_0 is the transition temperature of the bulk liquid, K_c is the cryoporometric constant of the liquid (determined by the V_M, molar volume, γ_{SL}, solid-liquid interfacial tension, ΔH, heat of melting and the T_0 of the liquid). r_p is the radius of the pore, which together with the n geometrical factor defines the specific surface (S) and the volume (V) of the pores. The detectable pore size range depends on the cryoporometry constant of the test liquid, its melting point, the thickness of the molten liquid layer in the frozen state, on the pore geometry, and last but not least on the technical conditions (the cooling capability of the cooler and type of NMR probe). The studied CA samples were measured in a fully saturated state with water as a pore filling liquid, for which the measurable pore size ranges from ca. 2 nm to 400 nm in diameter ($d_p = 2 \times r_p$, where r_p is the pore radius).

Details of the applied relaxation model:

The measured transversal (T_2) relaxation times were interpreted using the two-sites relaxation model, which involves two different types of water: (1) the adsorbed water (by physisorption or chemisorption) which is in fast exchange with (2) the bulk-like water inside a given water domain. Usually, the relaxation time of the adsorbed molecules cannot be measured on a carbon surface because of its high relaxation rate and low quantity (due to the high

hydrophobicity of the backbone), instead the measured T_2 value in partially or fully saturated pores is a volume-weighted average of the two domains according to the following equation:

$$\frac{1}{T_2} = \frac{V_s}{V}\frac{1}{T_{2,s}} + \frac{V_{bulk}}{V}\frac{1}{T_{2,bulk}}$$

Eq. S2

where V is the total volume of water, V_s is the volume of adsorbed water, V_{bulk} is the volume of pore filling bulk water, $T_{2,s}$ is the transversal time constant of adsorbed water, and T_{2bulk} is the transversal relaxation time of bulk phase water respectively.

The measured T_2 value depends on the pore size and the surface relaxivity according to Eq. S3.

$$\frac{1}{T_2} = \xi\frac{S_p}{V_p}\frac{1}{f^k} + \frac{1}{T_{2bulk}}$$

Eq. S3

where T_2 is the measured average transverse relaxation time, S_p is the surface area, V_p is the total volume of the pores, T_{2bulk} is the transversal relaxation time constant of the bulk liquid, ξ is the surface relaxation strength, describing the solid-liquid interface in the system. f is the filling factor in the case of partially filled pores, and can be defined as $(V_s + V_{bulk})/V_p$, where V_s is the volume of surface water participating in the exchange process with V_{bulk}, the volume of pore filling bulk water, while V_p is the total pore volume. k is an empiric coefficient characteristic for the mode of distribution of the liquid in the pore during the filling process and thus the saturation mechanism of the pores.[2] The value of k changes between 0 and 1; in the case of a uniform water distribution, where the entire surface layer is in direct contact and exchange with the bulk phase, k is equal to or close to 1; while k trends to 0 when the liquid layers are not in contact with the bulk phase, indicating a "plug-like" wetting mechanism. A simplified formula of Eq. S3 can be seen as Eq. 2. We have to note that in the case of CA30 and CA75 carbon aerogels the fitting error of the k parameter is somewhat higher than 10%, the reason for which is that here the model is applied for macropores with wide size distributions (see Fig. 10).

Since the effect of the surface is often considered uniform for the whole sample under study, the T_2 relaxation time constants report on the size of the confinement the liquid fills. Therefore, following the T_2 during the saturation of the pores reveals not only the detectable liquid domains, but their change in size and amount during the filling process as well.[3]

Figures:

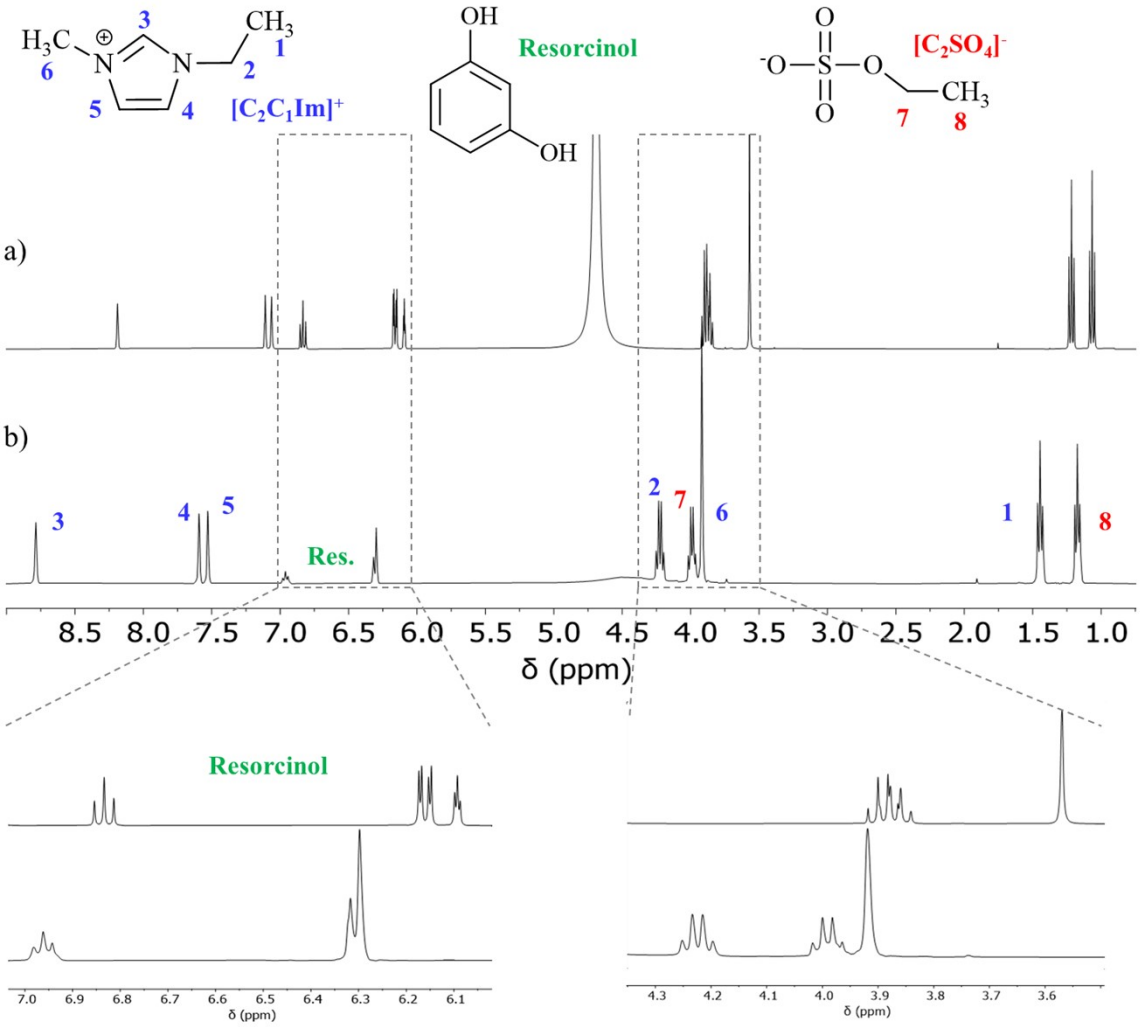

Fig. S1. The components of the studied system (above), the ^{1}H NMR spectra of resorcinol in the binary mixture of a) S30 and b) S75 with the identification of the signals, and two enlargements of the spectra ($[C_2C_1Im]^+$: blue; $[C_2SO_4]^-$: red; resorcinol: green).

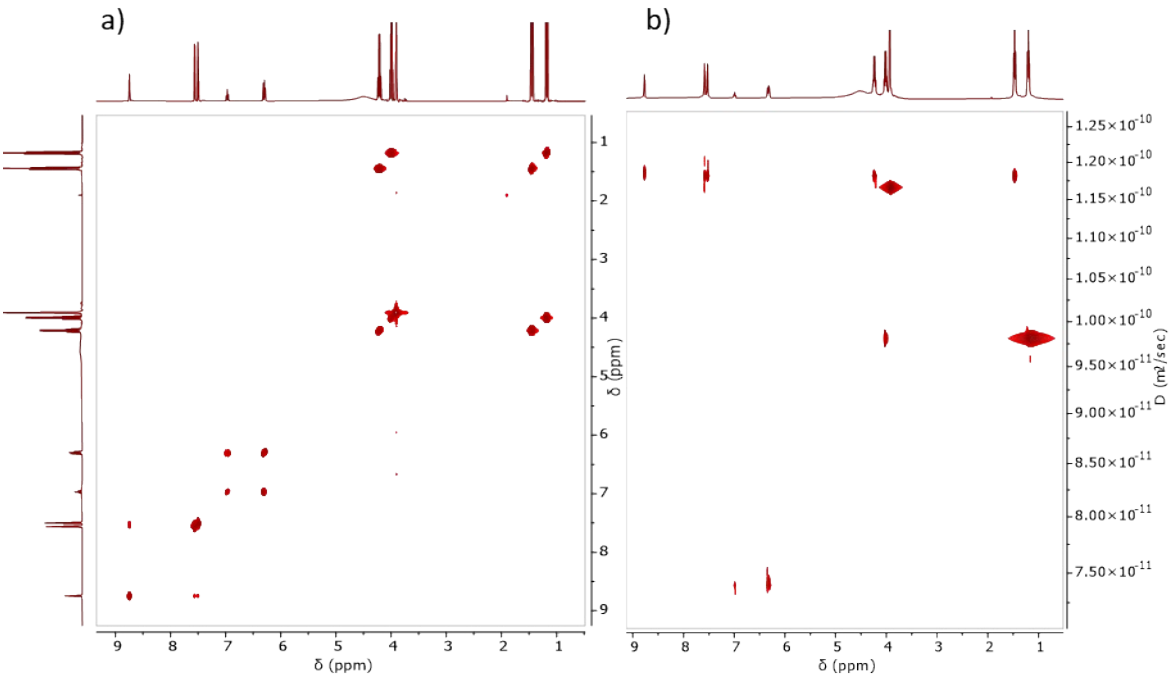

Fig. S2. 2D COSY (a) and DOSY (b) NMR spectra of resorcinol in the binary mixture of S75 composition. The COSY spectrum shows the protons on adjacent carbons, while DOSY assigns the protons of same diffusion coefficient.

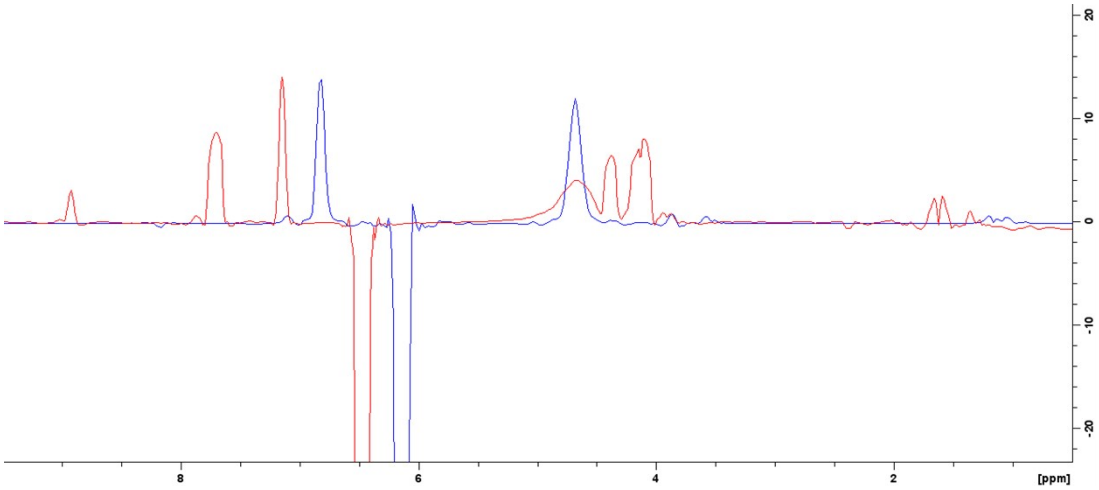

Fig. S3. Vertical 1D slices extracted from the NOESY spectra of the $[C_2C_1Im][C_2SO_4]$ – water – resorcinol system at S75 (red) and S30 (blue) compositions (Fig. 1.) at 6.3 and 6.16 ppm respectively (chemical shifts of resorcinol), (400 MHz, mixing time 800 ms, T=298 K). The slices are normalized to the crosspeaks of the resorcinol aromatic protons, and thus show the definitely higher intensity crosspeaks with all the other species in the high IL concentration solution (red curve).

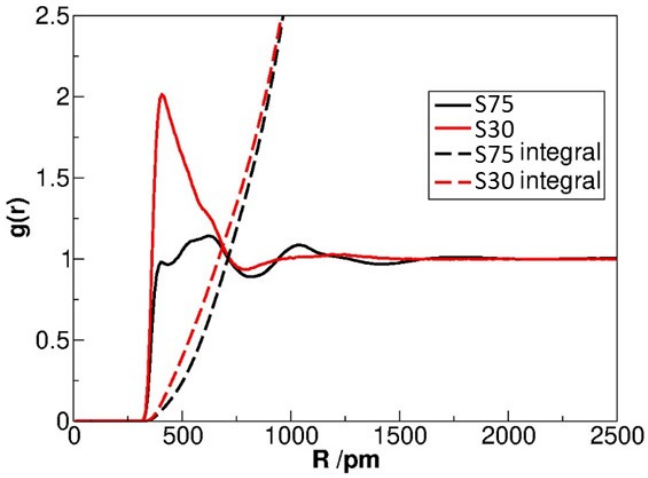

Fig. S4. Radial distribution functions defined between the centers of the aromatic rings of $[C_2C_1Im]^+$ and resorcinol in the $[C_2C_1Im][C_2SO_4]$ – water – resorcinol system at S75 and S30 compositions (75 and 30 wt% IL content) at 358 K.

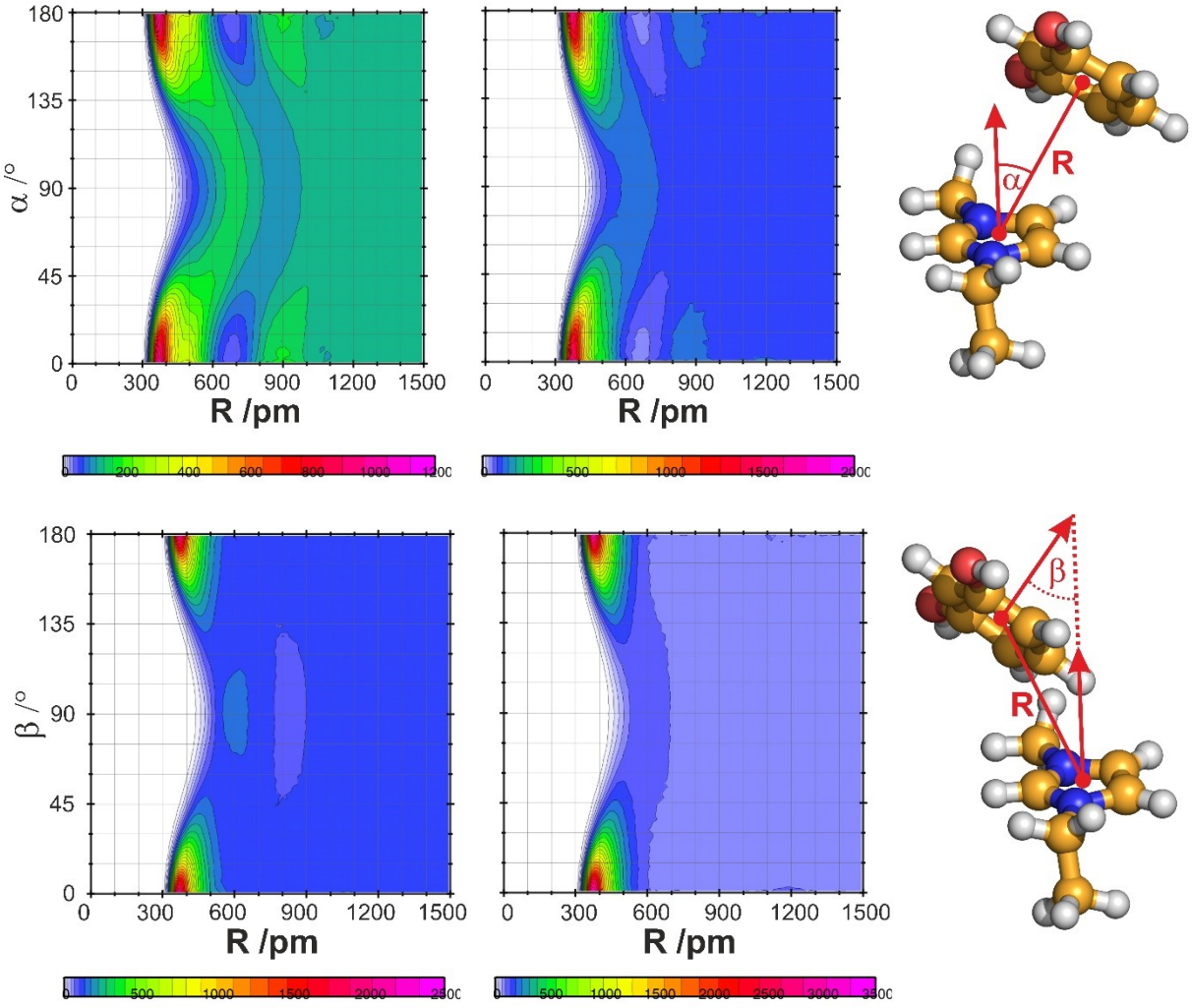

Fig. S5. Combined distribution functions correlating two directional angles (α, β) and the distance (R) of the aromatic ring centers of $[C_2C_1Im]^+$ and resorcinol in the $[C_2C_1Im][C_2SO_4]$ – water – resorcinol system (left: S75, right: S30) at 358 K.

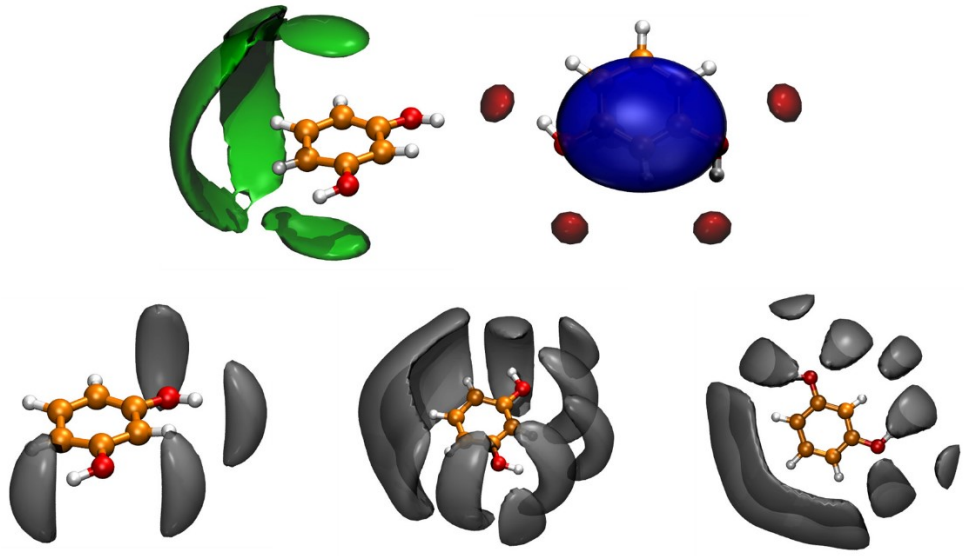

Fig. S6. Spatial distribution of the components in the $[C_2C_1Im][C_2SO_4]$ – water – resorcinol system (S30, 30 wt% IL) around resorcinol at 358 K ($[C_2C_1Im]^+$: blue; $[C_2SO_4]^-$: red; resorcinol: green; water: grey). Below, the distribution of water is shown at lower (left) and a higher (middle and right) occurrence cutoff values.

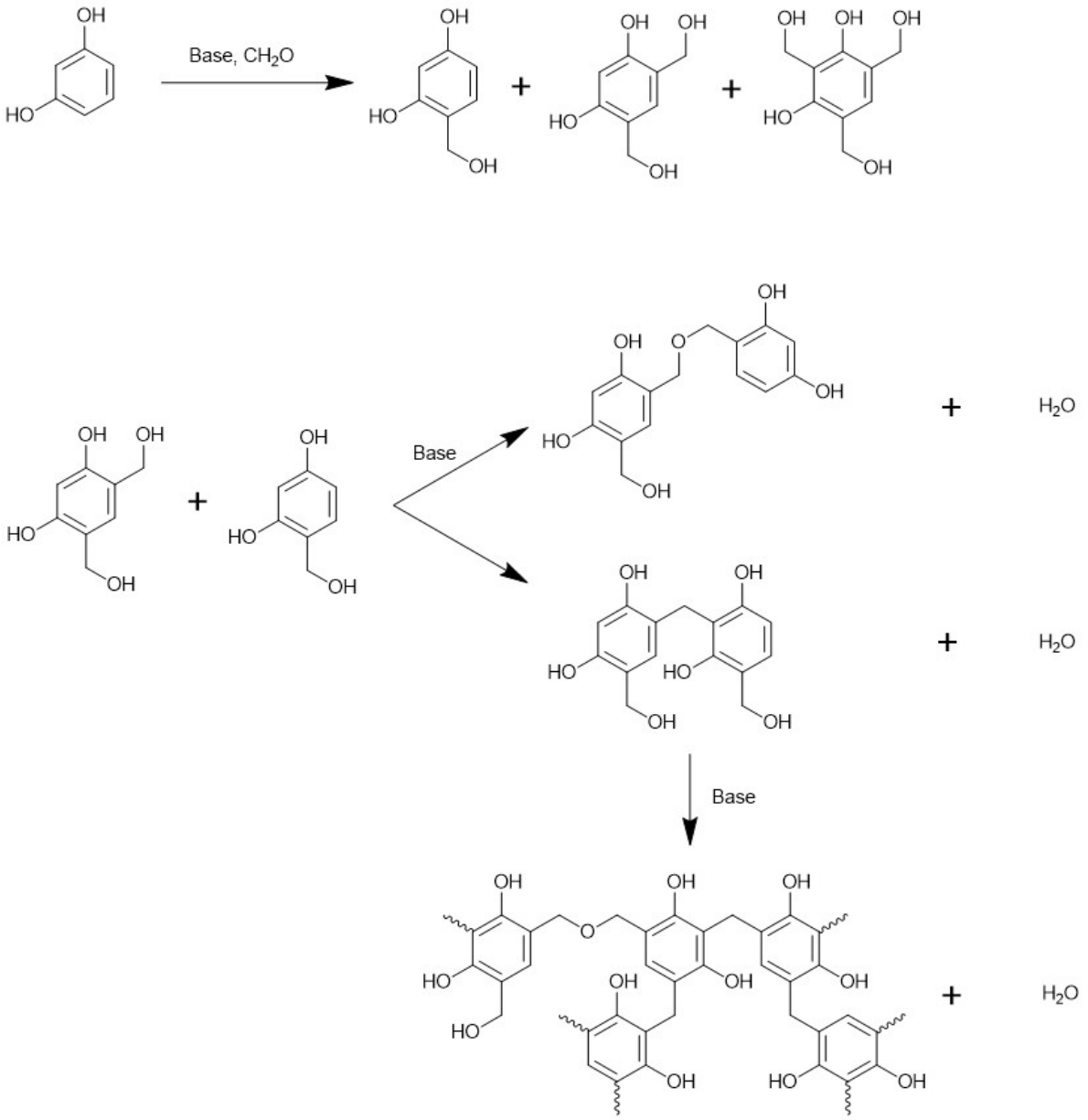

Fig. S7. The base-catalyzed reaction scheme of the polymerization of resorcinol by excess formaldehyde.[4]

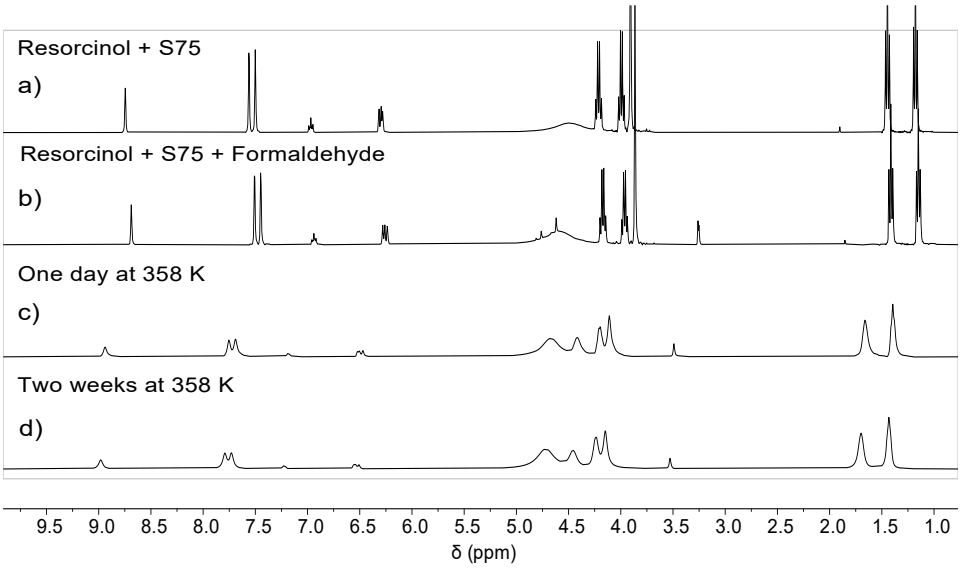

Fig. S8. ^{1}H NMR spectra of resorcinol in the S75 mixture (a), after addition of formaldehyde (S75+F) at 298 K (b), one day (c) and two weeks (d) later at 358 K.

Table S1. Self-diffusion coefficients (m^2/s) of the components in the studied samples, derived from the MD simulations (T = 358 K).

Sample	$[C_2C_1Im]^+$	$[C_2SO_4]^-$	Resorcinol	Oligomer
S30	1.66×10^{-9}	1.60×10^{-9}	1.30×10^{-9}	-
S75	8.11×10^{-11}	5.10×10^{-11}	4.54×10^{-11}	-
S0+P	-	-	3.24×10^{-9}	1.16×10^{-9}
S30+P	1.54×10^{-9}	1.53×10^{-9}	1.30×10^{-9}	2.98×10^{-10}
S75+P	7.52×10^{-11}	4.78×10^{-11}	4.37×10^{-11}	5.52×10^{-12}

We note that estimating dynamic properties for ionic liquid solutions is challenging for molecular dynamic simulations, often leading to significant underestimation of self-diffusion coefficients.[5-7] Nonetheless, the data show similar trends to the experimental results (see subsection 3.1.2) regarding the slowing effect of the oligomer on the diffusion of all species, and they confirm that higher IL concentration in the mixture decreases the diffusion coefficients of the species in the system.

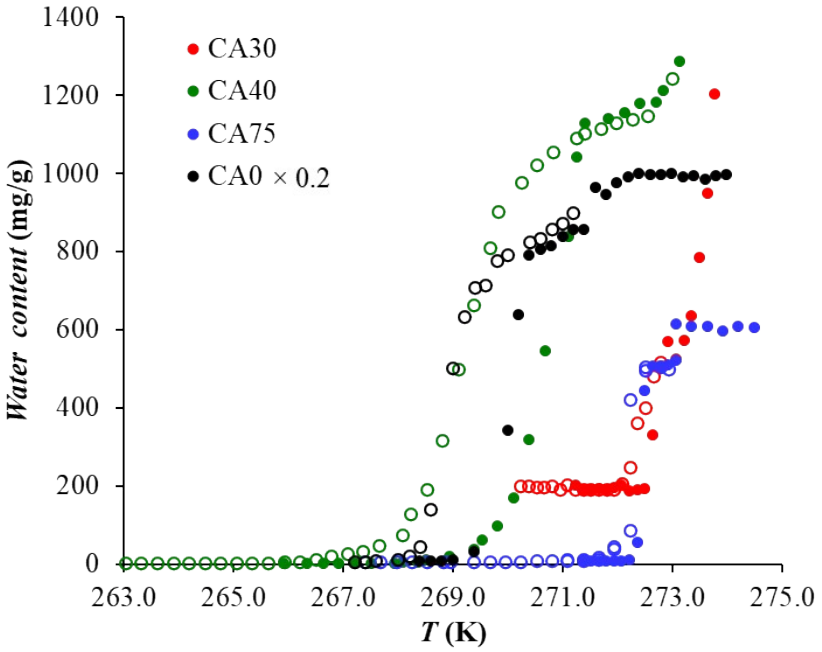

Fig. S9. Melting and freezing curves of the studied carbon aerogels from NMR cryoporometry. Empty and filled symbols stand for the freezing and melting processes, respectively. The water content values of CA0 are scaled by 0.2 for being represented on the same scale.

Characterization of CA40 [8]:

The carbon aerogel CA40 was prepared in 1-ethyl-3-methylimidazolium ethyl sulfate ($[C_2C_1Im][C_2SO_4]$, Sigma-Aldrich) – water binary solvent with ~40 wt% IL content (Table S1).

Table S2. The composition of the binary solvents used. The number in the acronym refers to the IL content in wt%.

Samples			$[C_2C_1Im][C_2SO_4]$ (wt%)	Water (wt%)	x_{IL}[a]	x_{water}[b]
Solution	Polymer aerogel	Carbon aerogel				
-	-	CA40[8]	40.7	42.6	0.07	0.93

[a,b]Molar fraction of IL and water in the binary solvent, respectively.

Cryoporometry measurements carried out on CA40 (Fig. S9), and the pore size distribution (Fig. S10.) revealed that this sample shows ordered mesoporous structure, similarly to CA0. The characteristic diameter is ~50 nm for CA40, while the distribution is monodisperse but somewhat wider (25-80 nm) than in the case of CA0. According to the derived data (Table S1) CA40 has a significant mesopore volume.

The measured T_2 relaxation times as a function of the water content (Fig. S11a) show the presence of the water layer, being formed from water clusters on the surface, similarly to S30 and S75. This additionally confirms that this feature can be observed for every studied carbon aerogel synthesized in IL — water mixture, regardless of the IL concentration. For CA40, containing monodisperse mesoporous pore systems, the T_2 values of the pore-filling water domain reach a saturation, indicating a complete filling at approximately 1 g/g water content, in accordance with the amount of water in the saturated mesopores from cryoporometry (Table S1). CA40 sample shows a k value of 0.66 (see fitting in Fig. S11b), revealing that more surface water takes part in the exchange process with the pore-filling domain than in the similarly mesoporous CA0.

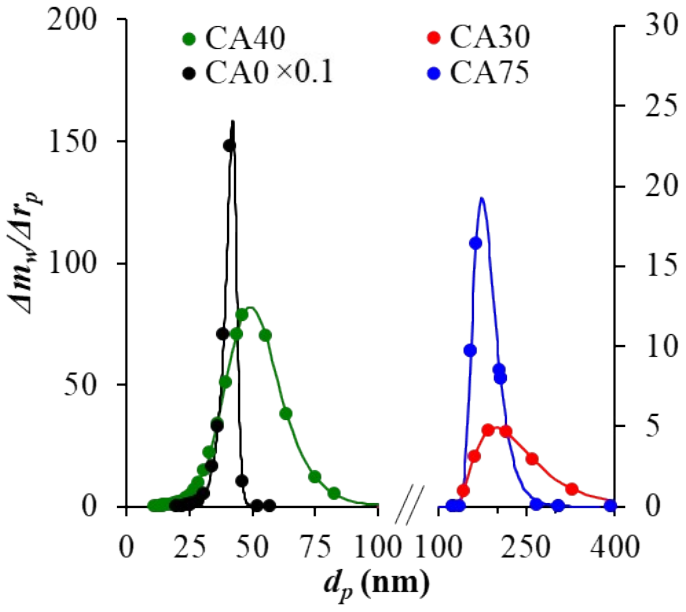

Fig. S10. Pore size distributions in RF carbon aerogel samples: CA0 (black)[8], CA30 (red), CA40 (green)[8], CA75 (blue), obtained from NMR cryoporometry (derived from the melting curves). Symbols show the measured data, while lines are calculated from the fitting of the melting curves. The intensity values of CA0 are scaled by 0.1 for being represented on the same scale.

Table S3. Morphological properties of the CA40 carbon aerogel saturated with water from NMR data.

Sample	d_p [a]	$m_{w,\,micro}$ [b]	$m_{w,\,meso}$ [c]	$m_{w,\,macro}$ [c]	k [d]
	nm	g/g	g/g	g/g	-
CA40 [8]	50	-	1.16	-	0.66 ± 0.07

[a] Pore diameter from NMR cryoporometry (maxima of the size distributions in Fig. S10); [b] water in micropores derived from the unfrozen signal; [c] water in saturated spherical meso- or macropores; [d] k parameter from relaxometry.

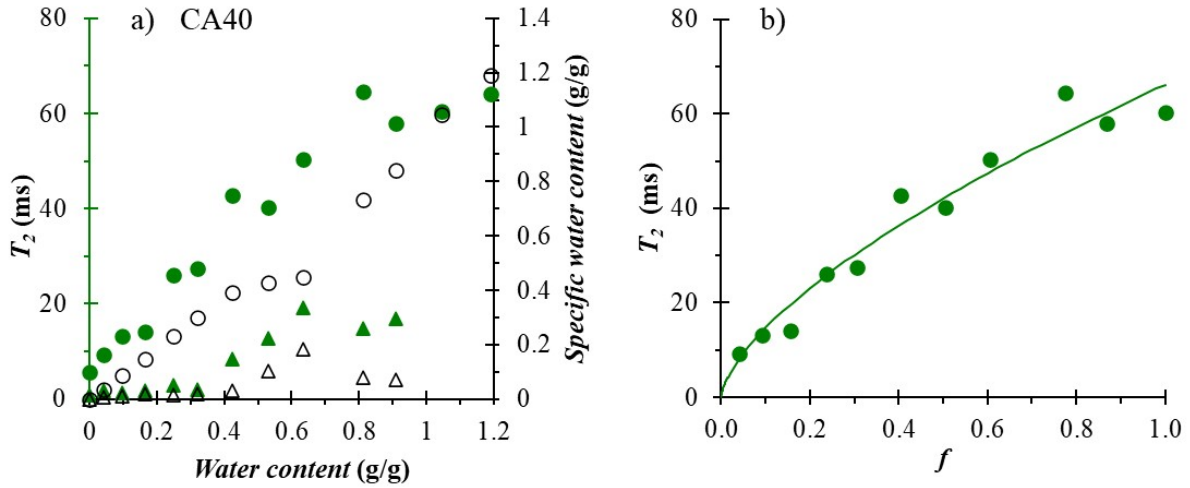

Fig. S11. Transversal (T_2) relaxation time (colored, filled) and specific water content (black, empty) as a function of the relative water content in CA40 [8] carbon aerogel sample. (a) ▲ and Δ stand for the adsorbed water clusters and water in micropores in contact with the pore wall, while ● and ○ visualize the pore-filling water. Transversal relaxation time as a function of the filling factor of the mesopores in CA40, with the fit of Eq. 4. (b)

The geometry of the oligomer structure applied in the MD simulation:

131

C	0.000000	0.000000	0.000000
H	0.000000	0.000000	1.070000
C	1.212436	0.000000	-0.700000
C	1.212436	0.000000	-2.100000
C	0.000000	0.000000	-2.800000
C	-1.212436	0.000000	-2.100000
C	-1.212436	0.000000	-0.700000
O	2.407551	0.000000	-0.010000
C	2.511474	0.000000	-2.850000
O	0.000000	0.000000	-4.180000
H	-2.155537	0.000000	-2.644500
H	-2.155537	0.000000	-0.155500
H	3.127346	0.000000	-0.625389
H	-0.892840	0.000000	-4.495667
H	2.315953	0.000000	-3.901985
H	3.072558	0.873651	-2.591508
O	3.235114	-1.126765	-2.516617
C	4.430230	-1.126765	-3.206617
C	5.216796	-2.351510	-2.844245
H	4.234709	-1.126765	-4.258602
H	4.991313	-0.253114	-2.948125
C	6.472773	-2.573058	-3.421685
C	7.206901	-3.716153	-3.083471
C	6.685052	-4.637701	-2.167816
C	5.429075	-4.416153	-1.590376
C	4.694947	-3.273058	-1.928590
O	6.987167	-1.664675	-4.324259
H	8.183872	-3.888485	-3.532637
O	7.408693	-5.764466	-1.834434
C	4.869951	-5.403525	-0.609317
H	3.717976	-3.100725	-1.479424
H	7.837591	-1.959351	-4.618801
H	6.919624	-6.279947	-1.208415
H	3.909071	-5.070576	-0.276519
H	4.772668	-6.358989	-1.081044
C	5.794233	-5.518215	0.566501
C	5.482080	-6.385457	1.620281
C	6.344743	-6.492501	2.717711
C	7.519560	-5.732302	2.761362
C	7.831712	-4.865060	1.707582
C	6.969049	-4.758017	0.610152
C	4.223349	-7.199955	1.573512
O	6.037050	-7.347354	3.756437
C	8.443842	-5.846992	3.937181
O	8.989746	-4.115722	1.750610
H	7.211860	-4.083426	-0.209538
H	9.051940	-3.585582	0.968374
H	6.716869	-7.302404	4.414187
H	9.282231	-5.197208	3.796526

H	7.922509	-5.568584	4.829146
C	8.923652	-7.262886	4.059761
C	9.440639	-7.723946	5.276374
C	9.888461	-9.045447	5.390782
C	9.819297	-9.905889	4.288577
C	9.302309	-9.444829	3.071963
C	8.854487	-8.123328	2.957555
O	9.508815	-6.875796	6.362834
C	10.442376	-9.539440	6.694297
H	10.167639	-10.933828	4.377570
C	9.228205	-10.366731	1.891029
O	8.344885	-7.668855	1.758322
H	9.879654	-7.338128	7.101438
H	8.367739	-8.368290	1.120297
H	10.731616	-10.564642	6.593295
O	11.542894	-8.783164	7.042587
H	9.694962	-9.453007	7.455087
C	12.052496	-9.237637	8.241820
C	13.248711	-8.415598	8.620396
H	11.305082	-9.151204	9.002610
H	12.341736	-10.262839	8.140819
C	13.939981	-8.690407	9.806409
C	15.056449	-7.923171	10.159747
C	15.481647	-6.881125	9.327072
C	14.790377	-6.606315	8.141060
C	13.673909	-7.373552	7.787722
O	13.520858	-9.717567	10.627188
H	15.594158	-8.136933	11.082295
H	16.350099	-6.284324	9.601919
H	15.121120	-5.795752	7.493358
O	12.992515	-7.102668	6.618652
H	14.090597	-9.771211	11.381727
H	12.269007	-7.706885	6.527727
H	4.153076	-7.798952	2.457348
H	3.377739	-6.546755	1.517176
O	4.246547	-8.019202	0.463243
C	3.088514	-8.768540	0.420216
C	3.113729	-9.659025	-0.786598
H	3.018241	-9.367536	1.304052
H	2.242904	-8.115340	0.363880
C	2.039153	-10.518394	-1.044998
C	2.062688	-11.349514	-2.171358
C	3.160799	-11.321264	-3.039318
C	4.235375	-10.461895	-2.780918
C	4.211840	-9.630775	-1.654558
H	1.184980	-10.540369	-0.369849
C	0.911356	-12.270266	-2.448215
O	3.183997	-12.140510	-4.149587
H	5.089548	-10.439920	-3.456067
O	5.271065	-8.783683	-1.399850
H	5.100366	-8.294298	-0.607276
H	3.989289	-12.001085	-4.627995
H	1.104227	-12.823214	-3.343731
C	0.743961	-13.220770	-1.299946
H	0.016611	-11.696096	-2.569289

C	-0.273381	-14.182091	-1.329588
C	-0.429616	-15.069228	-0.257870
C	0.431490	-14.995044	0.843489
C	1.448832	-14.033724	0.873131
C	1.605067	-13.146587	-0.198587
O	-1.122186	-14.255214	-2.415214
H	-1.220963	-15.816998	-0.280928
O	0.277487	-15.869508	1.899896
H	2.118650	-13.976020	1.729831
H	2.396414	-12.398817	-0.175530
H	-1.748457	-14.952545	-2.279851
H	0.933906	-15.688262	2.557979
H	8.809200	-9.844350	1.056492
C	10.606843	-10.843401	1.541542
H	8.610919	-11.206711	2.132468
C	10.792697	-11.719993	0.465882
C	12.079427	-12.164885	0.139695
C	13.180302	-11.733185	0.889167
C	12.994448	-10.856592	1.964827
C	11.707719	-10.411701	2.291014
O	9.707549	-12.145526	-0.272883
H	12.223995	-12.846749	-0.697015
O	14.448650	-12.171721	0.567639
H	13.850772	-10.520791	2.547809
H	11.563151	-9.729837	3.127724
H	10.001535	-12.729436	-0.958033
H	15.075688	-11.790319	1.166107

References:

1. Petrov, O. V.; Furó, I., NMR cryoporometry: Principles, applications and potential. *Progress in Nuclear Magnetic Resonance Spectroscopy* **2009,** *54* (2), 97-122.
2. Simina, M.; Nechifor, R.; Ardelean, I., Saturation-dependent nuclear magnetic resonance relaxation of fluids confined inside porous media with micrometer-sized pores. *Magnetic Resonance in Chemistry* **2011,** *49* (6), 314-319.
3. Maillet, B.; Sidi-Boulenouar, R.; Coussot, P., Dynamic NMR Relaxometry as a Simple Tool for Measuring Liquid Transfers and Characterizing Surface and Structure Evolution in Porous Media. *Langmuir* **2022,** *38* (49), 15009-15025.
4. Durairaj, R., *Resorcinol: Chemistry, Technology and Applications*. 2005.
5. Schröder, C., Comparing reduced partial charge models with polarizable simulations of ionic liquids. *Physical Chemistry Chemical Physics* **2012,** *14* (9), 3089-3102.
6. Hollóczki, O.; Malberg, F.; Welton, T.; Kirchner, B., On the origin of ionicity in ionic liquids. Ion pairing versus charge transfer. *Physical Chemistry Chemical Physics* **2014,** *16* (32), 16880-16890.
7. Kirchner, B.; Hollóczki, O.; Canongia Lopes, J. N.; Pádua, A. A. H., Multiresolution calculation of ionic liquids. *WIREs Computational Molecular Science* **2015,** *5* (2), 202-214.
8. Kéri, M.; Nyul, D.; László, K.; Novák, L.; Bányai, I., Interaction of resorcinol-formaldehyde carbon aerogels with water: A comprehensive NMR study. *Carbon* **2022,** *189*, 57-70.